Design Solutions for Reducing the Cogging Torque of PMSM

Tiberiu TUDORACHE[1], Mircea MODREANU[2]
[1]*University Politehnica of Bucharest, Bucharest, 060042, Romania*
[2]*Research Institute for Electrical Engineering (ICPE SA), Bucharest, 030138, Romania*
tudorach@amotion.pub.ro

Abstract—**This paper analyzes design solutions able to reduce the Cogging Torque (CT) amplitude of Permanent Magnet Synchronous Machines (PMSMs). The common point of these solutions is the particular constructions of the stator magnetic core from two concentric steel lamination stacks that leads to a closed stator slots structure in the air-gap region. The efficiency of the studied solutions is evaluated by Finite Element (FE) analysis for two different types of PMSMs: the first one with Surface Permanent Magnets (SPMs) and the second one with Interior Permanent Magnets (IPMs). The influence of the special stator constructions on the performances of the two types of machines is emphasized also in the paper, with positive and negative effects. This study proves that a PMSM whose stator magnetic core is designed as shown, leads to an important decrease of CT amplitude in comparison with a classical machine. Moreover, the studied design solutions may be mixed with other CT reduction methods so as to optimize the overall PMSM performance. A part of the numerical model results were experimentally validated.**

Index Terms—**cogging torque reduction, finite element method, permanent magnet machines.**

I. INTRODUCTION

One of the electrical machines increasingly used in small and medium power applications is the Permanent Magnet Synchronous Machine (PMSM) [1]-[5]. The replacement of classical electromagnetic excitation with Permanent Magnets (PMs) makes the PMSM a very efficient and reliable machine, with a large range of applications in several domains such as: industrial drive systems, electric propulsion, wind turbines, fly-wheel energy storage systems, etc. [6]-[11].

An important aspect that deserves a special attention during the design phase of PMSM is represented by the reduction of Cogging Torque (CT). CT is a parasitic torque that appears as a result of the magnetic attraction forces between Permanent Magnets (PMs) and stator teeth [12]. The presence of CT has several negative effects on the PMSM operation, such as: mechanical vibrations that may reduce the machine bearings lifetime, acoustic noise, positioning errors in case of precision systems, [13]-[15] etc.

The CT reduction represents a main subject for an important number of research papers published in the last years. Several design methods are recommended in these papers such as: optimum sizing of pole shape and stator teeth [12], [16], [17], adequate selection of number of poles

and slots [12], [18], skewing the stator core or PMs [12], [19], asymmetrical positioning of PMs or stator teeth [20]-[22], segmentation of PMs [23], filling the stator slots with magnetic wedges [19], shifting of slot openings [24] etc.

This paper analyzes a design solution able to drastically reduce the CT peak values of PMSM, applicable to both Surface Permanent Magnet (SPM) and Interior Permanent Magnet (IPM) constructions. This solution supposes a particular construction of the PMSM stator magnetic core of two concentric lamination stacks increasing thus the magnetic isotropy of the stator core in the airgap region [25].

The efficiency of the studied design solution is evaluated using the Finite Element Method (FEM), one of the most flexible and trustworthy numerical method that can be used for such purpose [26].

The physical support for the study is represented by two PMSMs with different constructions; the first one has the PMs glued on the rotor core (SPM construction) and the second one has the PMs inserted in the rotor core (IPM construction). Both PMSM structures use the same stator core geometry.

The detailed analysis presented in the paper emphasizes the advantages of the studied solution for CT reduction of PMSMs but also emphasizes the impact of that solution on the machine performance under no-load and load condition.

II. STUDIED DESIGN SOLUTION FOR CT REDUCTION OF PMSM

The design solution studied in the paper is able to reduce the CT amplitude by a particular construction of the stator core that is made of two concentric laminations stacks, keeping the rotor geometry unchanged, Fig. 1.

It is known that the CT appears due to the interaction between the PMs mounted on the rotor and the stator core with magnetic anisotropy (teeth and slots). Therefore a PMSM with slotless stator has a practically null CT, such constructions being already proposed in [27], [28]. However, compared to the slotted counterparts, the slotless PMSMs have typically larger airgaps to make room for the stator windings and larger PMs to reach the same magnetic flux density in the airgap.

The design solutions described in the paper are based on a compromise between slotted and slotless stator core PMSMs.

Unlike classical PMSMs, the studied solutions, with closed stator slots, have no slot openings towards the airgap, the resulting magnetic structure of the stator core being

nearly isotropic. However the magnetic isotropy of the stator core is not perfect because the thin magnetic bridges between adjacent teeth (inter-teeth bridges) may saturate during the machine operation since they become paths for the magnetic flux lines.

The different levels of magnetic saturation of the stator core regions (teeth, inter-teeth bridges) induce a slight magnetic anisotropy to the stator core that will entail small but non-null CT values. Thus in case of the studied design solutions it is expected that the CT amplitude decreases drastically but not to zero.

The stator core structure with closed slots can be obtained by several methods. The first method supposes to build the stator core as a single stack of laminations. Such a variant would clearly complicate the windings construction process and therefore will not be developed.

A second solution supposes to build the stator core of two lamination stacks. The inner laminations stack, Fig. 1a) includes the stator teeth and the inter-teeth bridges. The stator slots in this case are closed towards the air-gap by inter-teeth magnetic bridges, but opened towards the exterior to permit the insertion of the windings into the slots. The outer stator laminations stack, Fig. 1b) plays the role of a magnetic yoke for the stator core, being used also to close the slots after inserting the stator windings.

Depending on the technology used to separate the two laminations stacks (laser cutting, stamping/punching, electro-discharge) a small airgap layer may appear between the two parts but its thickness is very small.

The mechanical strength of the wounded stator can be increased by impregnation.

The thickness of inter-teeth bridges should not be very large because otherwise they may generate an important increase of the leakage magnetic flux and thus a reduction of the main magnetic flux of the machine. Too thin inter-teeth bridges are not recommended either, since the inner stack may fail from mechanical point of view during machine operation.

A third solution that leads to a similar effect as the second one is to build the stator core of two laminations stacks, the outer one, Fig. 1d) with open slots and the inner one, Fig. 1c) as a thin cylindrical crown used as an inter-teeth magnetic yoke in the air-gap region.

The last two design solutions applied to the PMSM have the merit of keeping practically unchanged the complexity of winding construction process.

The physical support for this study that aims to emphasize the advantages and the limitations of the analyzed solutions is represented by two machine configurations, the first one with SPMs, Fig. 2a) and the second one with IPMs, Fig. 2b).

The SPM machine is characterized by the following data: rated power 400 W, rated speed 1800 rpm, 10 poles, 36 slots, distributed winding, stator bore diameter 90 mm, stator outer diameter 128 mm, axial length 15 mm, no skewing. The IPM machine has practically the same main data but has only 12 stator slots and a concentrated single-tooth winding.
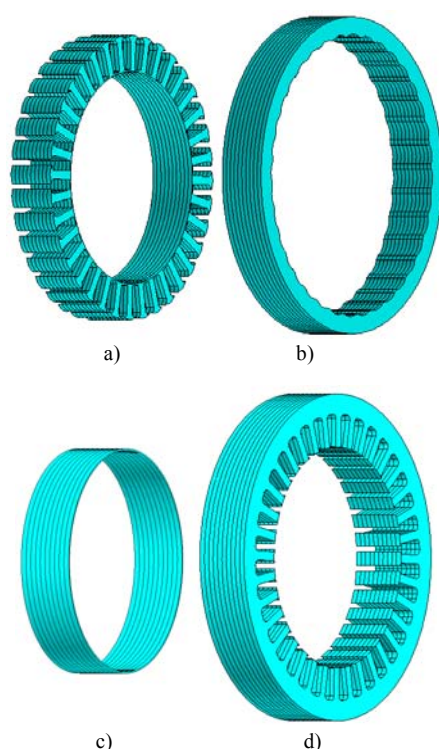

Figure 1. Stator core made of two distinct lamination stacks; a) inner lamination stack that includes the teeth and the inter-teeth bridges; b) outer lamination stack represented by the stator core yoke; c) inner cylindrical crown d) open slot stator magnetic core.

The outer and inner stator laminations stacks may be glued together (eventually using a ferromagnetic glue) to form a robust construction from mechanical point of view.
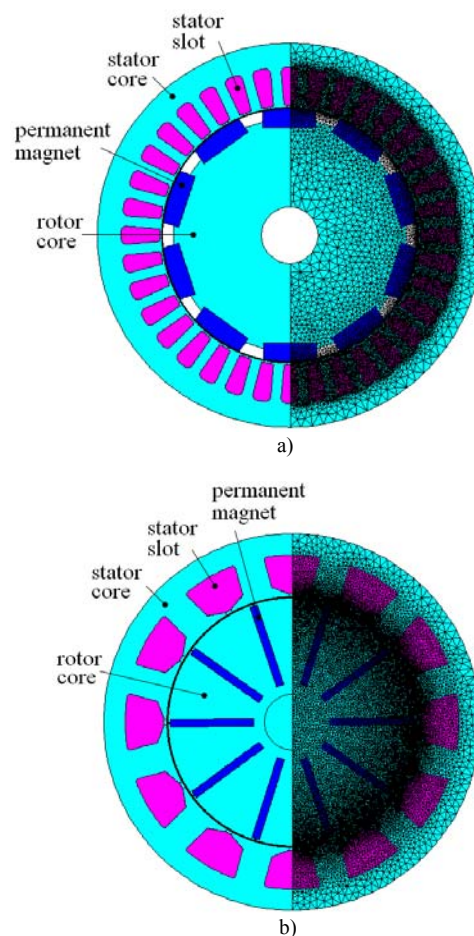

Figure 2. Cross section through the reference structures of the studied PMSMs and the corresponding FE mesh; a) SPM configuration; b) IPM configuration.

III.　　FEM COMPUTATION OF CT

One of the most accurate numerical methods that can be used for the computation of CT is the FEM.

The evaluation of CT oscillations of PMSM by FEM supposes first to solve a series of 2D magneto-static field problems for various rotor/stator relative positions and afterward, by post-processing the magnetic field solution, to compute the CT using the Virtual Work method [17].

The 2D FE computation domains for the CT computation are represented by cross sections through the studied PMSMs, Fig. 2.

The FE mesh consists of second order triangular elements with smaller size in the airgap region where three layers of finite elements were used for a good accuracy of CT calculation.

The partial differential equation characteristic to the magneto-static field problem associated to the studied PMSMs is given below [17]:

$$\nabla \times \left[\frac{1}{\mu} (\nabla \times \boldsymbol{A}) - \boldsymbol{H}_c \right] = 0 \qquad (1)$$

where $\boldsymbol{A}$ is the magnetic vector potential that has only one component A_z normally oriented to the computation plane, μ is the magnetic permeability of materials and $\boldsymbol{H}_c$ is the coercitive magnetic field strength of PMs.

The material properties of the SPM machine are the following: standardized magnetic steel laminations M600-50A for the stator core, NdFeB N35 for the PMs, regular steel for the rotor core.

The materials used in case of IPM machine are steel laminations M330-35A for the stator and rotor cores, regular steel for the rotor shaft and NdFeB N33 SH for the PMs.

The solution uniqueness of (1) supposes to specify a Dirichlet boundary conditions $\boldsymbol{A} = 0$ on the outer boundary of the 2D computation domain. In case of SPM machine a similar condition was applied on the inner boundary of rotor yoke.

The variation of CT computed for different rotor angular positions, for the two studied configurations, are shown in Fig. 3. The results are also summarized in Table I.

For each configuration (SPMs and IPMs) the CT results obtained for the closed slots stator core structure (2 lamination stacks, 2ST) are presented in comparison with those for the classical stator core structure (1 lamination stack, 1ST) with open slots, Fig. 3.
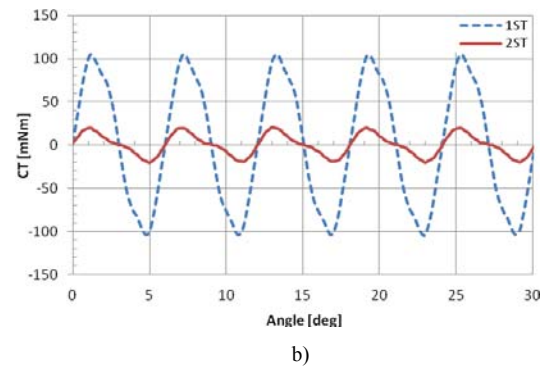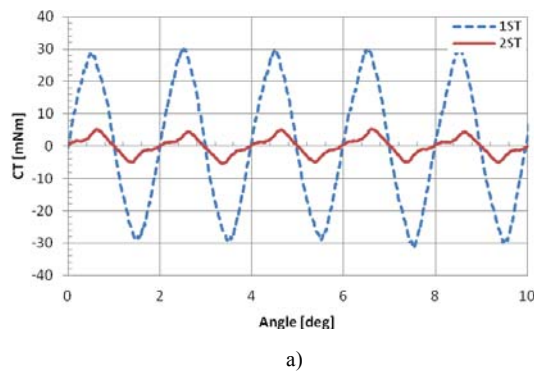

a)

b)

Figure 3. CT variation vs. rotor angular position obtained for classical stator core (made of 1 stack of laminations, 1ST) and for close slots stator core (made of 2 stacks of laminations, 2ST); a) SPM structure; b) IPM structure.

TABLE I. CT PEAK VALUES FOR SPM&IPM DESIGNS WITH 1&2 ST

	SPM 1 ST	SPM 2 ST	IPM 1 ST	IPM 2 ST
CT [mNm]	31.34	5.42	105.66	20.65
CT/RT*100 [%]	1.49	0.26	5.03	0.98

Studying the results in Table I we can notice that for closed slots stator core structure (2 ST), the CT peak value decreases for SPM structure from about 31.34 mNm to only 5.42 mNm (i.e. from 1.49 % to only 0.26 % of the rated torque) and for IPM from about 105.66 mNm to only 20.65 Nm (i.e. from 5.03 % to 0.98 % of the rated torque). The rated torque (RT) was estimated at approximately 2.1 Nm.

IV.　　IMPACT OF STATOR CORE STRUCTURE ON PMSMS OPERATION. VALIDATION OF FE MODEL

We emphasized so far the effect of the closed slots stator core structure on the CT values of PMSMs. Now we are interested in studying the impact of this solution on the operation characteristics of SPM and IPM machines. The quantities that are taken into account for the two studied machines are the no-load e.m.f. waveform and the electromagnetic torque.

For analyzing these quantities, (1) should be completed so as to include the current density $\boldsymbol{J}_s$ (in case of CT computation $\boldsymbol{J}_s$ was null) flowing through the stator slots, as a source of magnetic field:

$$\nabla \times \left[\frac{1}{\mu} (\nabla \times \boldsymbol{A}) - \boldsymbol{H}_c \right] = \boldsymbol{J}_s \qquad (2)$$

Eq. (2) is underdetermined; it has two unknowns, the state variable $\boldsymbol{A}$ and the quantity $\boldsymbol{J}_s$ which is apriori unknown ($\boldsymbol{J}_s$ depends on the machine load). In order to solve (2) the FE model of the machine should be coupled with an associated circuit model as shown in Fig. 4.

The no-load operation is simulated by imposing a high value to the RLu, RLv and RLw resistances, the rotor speed being set at 1800 rpm. The waveforms of no-load e.m.f. for the SPM and IPM machines are presented in Fig. 5.

Studying these results we can notice that in comparison with the open slot stator structure, by using the close slots stator construction, the r.m.s. value of e.m.f. decreases from 23.05 V to 21.34 V (i.e. a decrease of 7.42%) in case of SPM machine and from 23.92 V to 21.5 V (i.e. a decrease of 10.12%) in case of IPM machine.
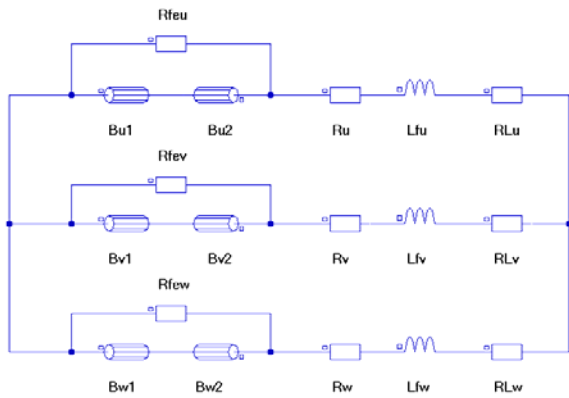
Figure 4. Circuit model associated to the FE model of the PMSM; Bu1, Bu2, ... Bw2 - positively and negatively coil sides of U, V and W phases; Rfeu, Rfev, Rfew - resistances that model the iron losses; Ru, Rv, Rw - phase resistances; Lfu, Lfv, Lfw - frontal end inductances; RLu, RLv, RLw - load resistances.
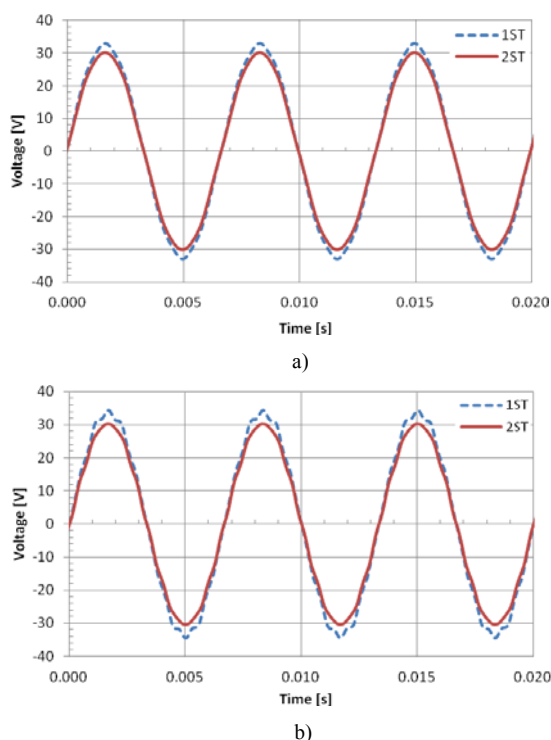

a)

b)

Figure 5. Waveforms of no-load e.m.f. for the studied PMSMs in case of classical stator core (made of 1 stack of laminations, 1ST) and in case of closed slots stator core (made of 2 stacks of laminations, 2ST); a) SPM structure; b) IPM structure.

In case of SPM machine the e.m.f. waveform obtained for the close slots stator construction has a similar shape to that of the classical stator but with a small decrease in amplitude.

In case of IPM machine the e.m.f. waveform obtained for the close slots stator construction is closer to a sinusoidal function than for the classical construction, the FFT analysis revealing smaller amplitudes of the 7th (0.47% vs. 1.11%) and 11th (1.36% vs. 2.21%) order harmonics.

By simulating the load regime of the SPM and IPM machines, operating as motor in the same conditions (in this case the circuit in Fig. 4 should be completed with two current sources per two phases), at the same r.m.s. current per phase of 5.5 A, we obtained the time dependence of electromagnetic torque for the classical and close slots stator constructions as shown in Fig. 6.
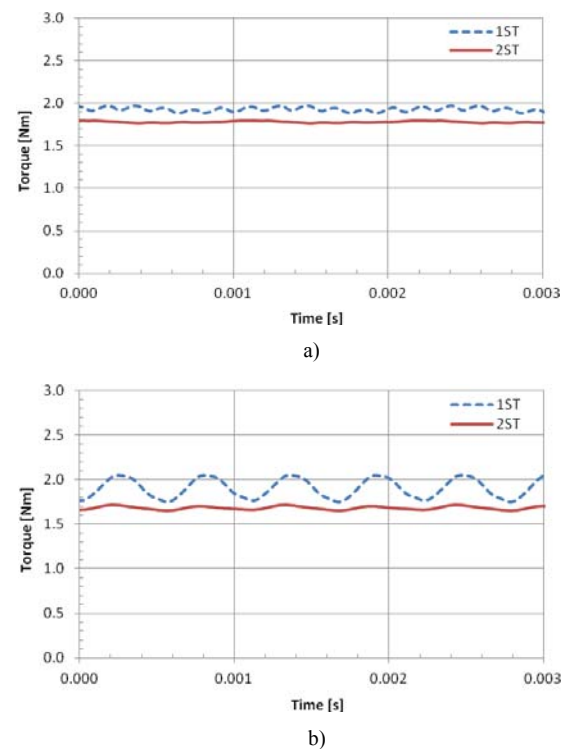

a)

b)

Figure 6. Electromagnetic torque oscillations for PMSMs with stator core with one (1ST) and two (2ST) stacks of laminations; a) SPM structure; b) IPM structure.

The numerical results prove that the closed slots stator construction entails smoother oscillations of the electromagnetic torque in both studied cases, but at the price of a slight reduction of the mean values of the electromagnetic torque from 1.93 Nm to 1.78 Nm for SPM machine and from 1.91 Nm to 1.68 Nm for IPM machine.

By using the closed slots stator construction we can notice a decrease of 7.8 % of electromagnetic torque in case of IPM machine and 12 % decrease in case of SPM. Despite this inconvenient the closed slots stator construction lead to a much more prominent CT reduction. Thus the studied stator design may be used in applications where small CT peak values are essential (high precision drive systems, wind turbines etc.).

The experimental validation of the FE model was done by comparing the computed e.m.f. waveform with those obtained by laboratory measurements in case of the IPM machine shown in Fig. 7.

A good concordance between the experimental and numerical results can be remarked in Fig. 8.

V. INFLUENCE OF THICKNESS OF INTER-TEETH MAGNETIC BRIDGES

An important geometrical parameter associated to the close slots stator structure of PMSM, that may affect the machine performance in no-load/load condition, is the thickness of the inter-teeth magnetic bridges. A very small thickness of this region is not recommended since it may weaken the mechanical resistance of the stator assembly while a very large thickness is not adequate either, since it increases the leakage magnetic flux, the leakage reactance of the machine and thus decreases the machine power factor.

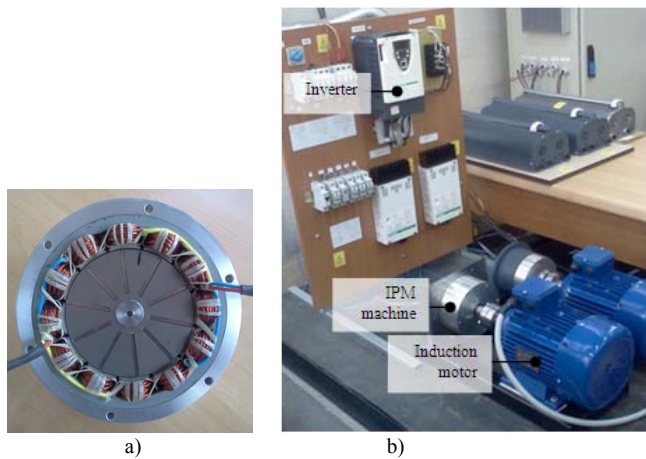a)   b)

Figure 7. Experimental validation setup; a) Experimental model of IPM machine; b) experimental setup used for testing the IPM machine.
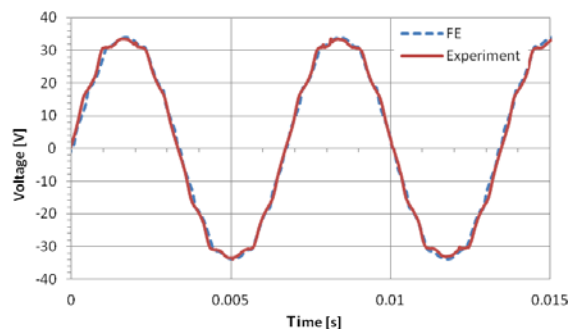

Figure 8. Waveforms of no-load e.m.f. obtained by FE analysis and by experimental measurements.

The effect of inter-teeth magnetic bridge thickness on PMSM performance was analyzed by a series of FE computations for different values of this parameter in the range 0.5 mm and 2 mm. The numerical results of CT, electromagnetic torque and no-load e.m.f. are presented in Figs. 9 to 12.

The results in Fig. 9 prove that in case of IPM machine by increasing the thickness of the inter-teeth magnetic bridge in the studied range, the peak value of CT decreases drastically, about 10 times. In case of the SPM machine the decrease of CT is less important (about 3.92 times) and the CT has a local minimum point for around 0.62 mm thickness (1.21 mNm); this thickness was used for the simulations presented previously. After that minimum point there is a relatively flat region for the CT, the smallest CT value (1 mNm) being obtained for 2 mm thickness.

The results shown in Fig. 10 show that the dependence between the mean value of electromagnetic torque and inter-teeth magnetic bridge thickness has a decreasing trend and it is similar in case of the SPM and IPM machines. The decrease of electromagnetic torque is of about 14.93% in case of SPM machine and only 12.58% in case of IPM machine.

By studying the graphical results in Fig. 11 we can remark that in case of SPM machine the curve e.m.f. (r.m.s. value) versus thickness of inter-teeth magnetic bridge has also a decreasing trend; the e.m.f. value drops from 21.57 V (for a thickness of 0.5 mm) to only 16.28 V (for a thickness of 2 mm), i.e. a 24.53 % decrease.
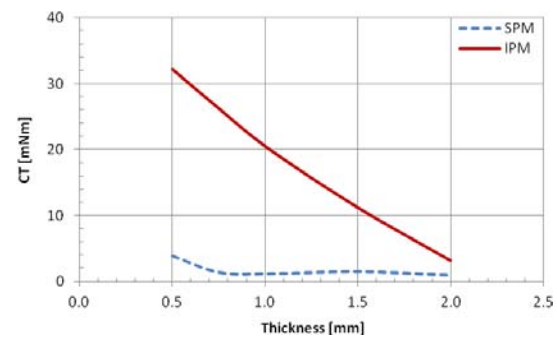

Figure 9. CT peak value versus thicknesses of inter-teeth magnetic bridges in case of SPM and IPM machines.
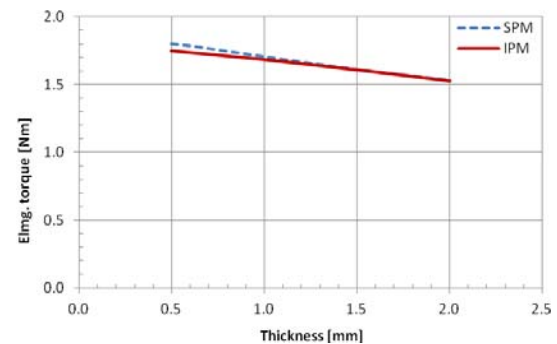

Figure 10. Electromagnetic torque versus thicknesses of inter-teeth magnetic bridges in case of SPM and IPM machines.
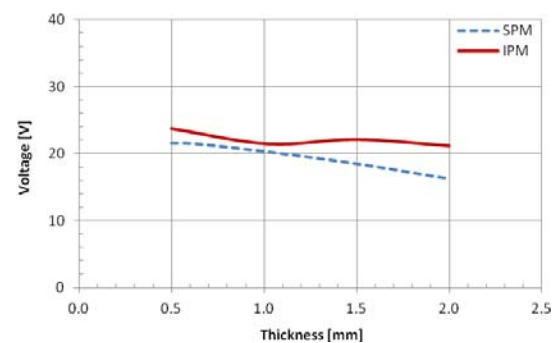

Figure 11. R.m.s. value of E.m.f. versus thicknesses of inter-teeth magnetic bridges in case of SPM and IPM machines.

In case of IPM machine the e.m.f decreases with 10.58 %, from 23.72 V to 21.21 V. The e.m.f. has a local minimum point (e.m.f. of 21.5 V) for a thickness of about 1.1 mm, then it increases and decreases again.

We can conclude that the close slots PMSM design both in SPM and IPM configuration lead to a very important CT peak value decrease at the price of a slight decrease of the electromagnetic torque and of the r.m.s. value of e.m.f.

VI. CONCLUSIONS

This paper analyzes a close stator slots design for PMSMs able to drastically reduce the CT peak values. The studied solution supposes to build the stator core of two distinct lamination stacks. The design solution was applied to a SPM and to a IPM machine, the peak value of CT decreasing in both cases about five times, Table I.

The impact of the close slots design on the PMSM performance was also analyzed. The numerical results showed that by using this design, a small decrease of the electromagnetic torque value and of the r.m.s. value of e.m.f. is obtained both in case of SPM and IPM machines.

The influence of inter-teeth magnetic bridge thickness in case of closed stator slots design was also studied. Higher decrease rates of CT peak values are generally obtained for larger values of inter-teeth magnetic bridge thickness for both SPM and IPM machines but at the price of a decrease of electromagnetic torque and of the r.m.s. value of e.m.f.

The studied PMSM design solution, with closed stator slots, can be applied also in combination with other CT reduction methods such as slots skewing, PMs skewing, asymmetrical placement of PMs etc.

A part of the FE numerical results obtained for the IPM machine were experimentally validated.

REFERENCES

[1] Y.A.-R.I. Mohamed, "Direct Instantaneous Torque Control in Direct Drive Permanent Magnet Synchronous Motors—a New Approach", IEEE Trans. Energy Convers., vol. 22, no. 4, pp. 829- 838, 2007. [Online]. Available: http://dx.doi.org/10.1109/TEC.2007. 895869

[2] G. Patterson, T. Koseki, Y. Aoyama, K. Sako, "Simple Modeling and Prototype Experiments for a New High-Thrust Low-Speed Permanent-Magnet Disk Motor", IEEE Trans. Ind. Appl., vol. 47, no. 1, pp. 65- 71, 2011. [Online]. Available: http://dx.doi.org/10.1109/ TIA.2010. 2090933

[3] Y. Inoue, Y. Kawaguchi, S. Morimoto, M. Sanada, "Performance Improvement of Sensorless IPMSM Drives in a Low-Speed Region Using Online Parameter Identification", IEEE Trans. Ind. Appl., vol. 47, no. 2, pp. 798- 804, 2011. [Online]. Available: http://dx.doi.org/ 10.1109/TIA.2010.2101994

[4] P. Curiac, Do Hyun Kang, "Preliminary Evaluation of a Megawatt-Class Low-Speed Axial Flux PMSM With Self-Magnetization Function of the Armature Coils", IEEE Trans. Energy Convers., vol. 22, no. 3, pp. 621- 628, 2007. [Online]. Available: http://dx.doi. org/10.1109/TEC.2007.895876

[5] P. Zheng, Y. Sui, J. Zhao, C. Tong, T.A. Lipo, A. Wang, "Investigation of a Novel Five-Phase Modular Permanent-Magnet In-Wheel Motor", IEEE Trans. Magn., vol. 47, no. 10, 2011, pp. 4084-4087. [Online]. Available: http://dx.doi.org/10.1109/TMAG.2011. 2150207

[6] T. Herold, E. Lange, K. Hameyer, "System Simulation of a PMSM Servo Drive Using Field-Circuit Coupling", IEEE Trans. Magn., vol. 47, no. 5, 2011, pp. 938 - 941. [Online]. Available: http://dx.doi.org/ 10.1109/TMAG.2010.2090866

[7] P. Zheng, J. Zhao, R. Liu, C. Tong, Q. Wu, "Magnetic Characteristics Investigation of an Axial-Axial Flux Compound-Structure PMSM Used for HEVs", IEEE Trans. Magn., vol. 46, no. 6, 2010, pp. 2191 - 2194. [Online]. Available: http://dx.doi.org/10.1109/TMAG.2010. 2042042

[8] M. Hafner, T. Finken, M. Felden and K. Hameyer, "Automated Virtual Prototyping of Permanent Magnet Synchronous Machines for HEVs", IEEE Trans. Magn., vol. 47, no. 5, pp. 1018 - 1021, 2011. [Online]. Available: http://dx.doi.org/10.1109/TMAG.2010.2091675

[9] T.D. Batzel, K.Y. Lee, "Electric propulsion with the sensorless permanent magnet synchronous motor: model and approach", IEEE Trans. Energy Convers., vol. 20, no. 4, pp. 818- 825, 2005. [Online]. Available: http://dx.doi.org/10.1109/TEC.2005.847948

[10] J. Sopanen, V. Ruuskanen, J. Nerg and J. Pyrhonen, "Dynamic Torque Analysis of a Wind Turbine Drive Train Including a Direct-Driven Permanent Magnet Generator", Trans. Ind. Electron., vol. 58, no. 9, 2010, pp. 3859 - 3867. [Online]. Available: http://dx.doi.org/ 10.1109/TIE.2010.2087301

[11] D.J. You, S.M. Jang, J.P. Lee, T.H. Sung, "Dynamic Performance Estimation of High-Power FESS Using the Operating Torque of a PM Synchronous Motor/Generator", IEEE Trans. Magn., vol. 44, no. 11, pp. 4155- 4158, 2008. [Online]. Available: http://dx.doi.org/10.1109/ TMAG.2008.2002607

[12] N. Bianchi, S. Bolognani, "Design Techniques for Reducing the Cogging Torque in Surface-Mounted PM Motors", IEEE Trans. Ind. Appl., vol. 38, no. 5, pp. 1259 - 1265, 2002. [Online]. Available: http://dx.doi.org/10.1109/TIA.2002.802989

[13] R. Islam, I. Husain, "Analytical Model for Predicting Noise and Vibration in Permanent-Magnet Synchronous Motors", IEEE Trans.

Ind. Appl., vol. 46, no. 6, pp. 2346- 2354, 2010. [Online]. Available: http://dx.doi.org/10.1109/TIA.2010.2070473

[14] E. Muljadi and J. Green, "Cogging Torque Reduction in a Permanent Magnet Wind Turbine Generator", Proc. of the American Society of Mechanical Engineers Wind Energy Symposium, Reno, Nevada, USA, 2002.

[15] T. Tudorache, R. Ben Ayed, S. Brisset, M. Popescu, "Cogging Torque Reduction of PMSM using Optimization Algorithms", Proc. of International Symposium on Electromagnetic Fields in Mechatronics, Electrical and Electronic Engineering (ISEF 2011), Madeira, Portugal, 2011.

[16] A. Jabbari, M. Shakeri, A.S. Gholamian, "Rotor Pole Shape Optimization of Permanent Magnet Brushless DC Motors Using the Reduced Basis Technique", Advances in Electrical and Computer Engineering Journal, Vol. 9, No. 2, pp. 75-81, 2009. [Online]. Available: http://dx.doi.org/10.4316/aece.2009.02012

[17] A. Jabbari, M. Shakeri, A. Nabavi Niaki, "Iron Pole Shape Optimization of IPM Motors Using an Integrated Method", Advances in Electrical and Computer Engineering Journal, Vol. 10, No. 1, pp. 67-70, 2010. [Online]. Available: http://dx.doi.org/10.4316/aece.2010. 01012

[18] T. Tudorache and M. Popescu, "Optimal Design Solutions for Permanent Magnet Synchronous Machines", Advances in Electrical and Computer Engineering Journal (AECE), vol. 11, no. 4, pp. 77-82, 2011. [Online]. Available: http://dx.doi.org/10.4316/aece.2011.04012

[19] T. Tudorache, L. Melcescu and M. Popescu, "Methods for Cogging Torque Reduction of Directly Driven PM Wind Generators", Proc. of International Conference on Optimization of Electric and Electronic Equipment (OPTIM 2010), Moieciu, Romania, 2010. [Online]. Available: http://dx.doi.org/10.1109/OPTIM.2010.5510390

[20] D. Wang, X. Wang, D. Qiao, Y. Pei, S.-Y. Jung, "Reducing Cogging Torque in Surface-Mounted Permanent-Magnet Motors by Nonuniformly Distributed Teeth Method", IEEE Trans. Magn., vol. 47, no. 9, pp. 2231 - 2239, 2011. [Online]. Available: http://dx.doi.org /10.1109/TMAG.2011.2144612

[21] S.M. Hwang, J.B. Eom, G.B. Hwang, W.B. Jeong and Y.H. Jung, "Cogging torque and acoustic noise reduction in permanent magnet motors by teeth pairing", IEEE Trans. Magn., vol. 36, no. 5, pp. 3144 - 3146, 2000. [Online]. Available: http://dx.doi.org/10.1109/20. 908714

[22] D. Wang, X. Wang, Y. Yang and R. Zhang, "Optimization of Magnetic Pole Shifting to Reduce Cogging Torque in Solid-Rotor Permanent-Magnet Synchronous Motors", IEEE Trans. Magn., vol. 46, no. 5, pp. 1228 - 1234, 2010. [Online]. Available: http://dx.doi. org/10.1109/TMAG.2010.2044044

[23] M. Ashabani, Y.A.-R.I. Mohamed, "Multiobjective Shape Optimization of Segmented Pole Permanent-Magnet Synchronous Machines With Improved Torque Characteristics", IEEE Trans. Magn., vol. 47, no. 4, pp. 795 - 804, 2011. [Online]. Available: http://dx.doi.org/10.1109/TMAG.2010.2104327

[24] S.A. Saied, K. Abbaszadeh, "Cogging Torque Reduction in Brushless DC Motors Using Slot-Opening Shift", Advances in Electrical and Computer Engineering Journal, Vol. 9, No. 1, pp. 28-33, 2009. [Online]. Available: http://dx.doi.org/10.4316/aece.2009. 01005

[25] T. Tudorache, M. Popescu, "Methods for Reducing the Parasitic Torque in a Permanent Magnet Synchonous Machine", Romanian Patent no. RO126618-A2, 2011.

[26] J.A. Güemes, A.A. Iraolagoitia, J.J. Del Hoyo, P. Fernández, "Torque Analysis in Permanent-Magnet Synchronous Motors: A Comparative Study", IEEE Trans. Energy Convers., vol. 26, no. 1, pp. 55- 63, 2011. [Online]. Available: http://dx.doi.org/10.1109/TEC.2010. 2053374

[27] T.D. Batzel, K.Y. Lee, "Slotless permanent magnet synchronous motor operation without a high resolution rotor angle sensor", IEEE Trans. Energy Convers., vol. 15, no. 4, pp. 366- 371, 2000. [Online]. Available: http://dx.doi.org/10.1109/60.900494

[28] P.D. Pfister, Y. Perriard, "Very-High-Speed Slotless Permanent-Magnet Motors: Analytical Modeling, Optimization, Design, and Torque Measurement Methods", IEEE Trans. Ind. Electron., vol. 57, no. 1, pp. 296- 303, 2010. [Online]. Available: http://dx.doi.org/ 10.1109/TIE.2009.2027919